Original Article

Deep Learning-based Lung dose Prediction Using Chest X-ray Images in Non-small Cell Lung Cancer Radiotherapy

Takahiro Aoyama, Hidetoshi Shimizu, Yutaro Koide, Hidemi Kamezawa[1], Jun-Ichi Fukunaga[2], Tomoki Kitagawa, Hiroyuki Tachibana, Kojiro Suzuki[3], Takeshi Kodaira

Department of Radiation Oncology, Aichi Cancer Center, Nagoya, [1]Division of Radiological Sciences, Graduate School of Health Sciences, Teikyo University, Fukuoka, [2]Division of Radiology, Department of Medical Technology, Kyushu University Hospital, Fukuoka, [3]Department of Radiology, Aichi Medical University, Nagakute, Aichi, Japan

Abstract

Purpose: This study aimed to develop a deep learning model for the prediction of V_{20} (the volume of the lung parenchyma that received ≥20 Gy) during intensity-modulated radiation therapy using chest X-ray images. **Methods:** The study utilized 91 chest X-ray images of patients with lung cancer acquired routinely during the admission workup. The prescription dose for the planning target volume was 60 Gy in 30 fractions. A convolutional neural network-based regression model was developed to predict V_{20}. To evaluate model performance, the coefficient of determination (R^2), root mean square error (RMSE), and mean absolute error (MAE) were calculated with conducting a four-fold cross-validation method. The patient characteristics of the eligible data were treatment period (2018–2022) and V_{20} (19.3%; 4.9%–30.7%). **Results:** The predictive results of the developed model for V_{20} were 0.16, 5.4%, and 4.5% for the R^2, RMSE, and MAE, respectively. The median error was −1.8% (range, −13.0% to 9.2%). The Pearson correlation coefficient between the calculated and predicted V_{20} values was 0.40. As a binary classifier with V_{20}<20%, the model showed a sensitivity of 75.0%, specificity of 82.6%, diagnostic accuracy of 80.6%, and area under the receiver operator characteristic curve of 0.79. **Conclusions:** The proposed deep learning chest X-ray model can predict V_{20} and play an important role in the early determination of patient treatment strategies.

Keywords: Chest X-ray, convolutional neural network, lung cancer radiotherapy, lung dose

Received on: 15-09-2023 **Review completed on:** 29-01-2024 **Accepted on:** 29-01-2024 **Published on:** 30-03-2024

Introduction

Radiation-induced pneumonia (RP) is a major adverse event following radiotherapy in patients with lung cancer. Intensity-modulated radiation therapy (IMRT) is a known promising treatment for reducing RP,[1] and the incidence of RP of grade ≥3 was lower with IMRT in a phase III study for locally advanced lung cancer.[2] Durvalumab after concurrent chemoradiation therapy for locally advanced nonsmall cell lung cancer (NSCLC) has been established as the standard treatment;[3] however, patients with grade ≥2 pneumonia after chemoradiation therapy are not eligible for durvalumab therapy. Therefore, providing radiotherapy that does not cause RP grade ≥2 is necessary.

Recently, machine learning techniques have been widely used to predict pneumonia.[4,5] Specifically, many studies have been conducted to predict pneumonia using chest X-ray images with deep learning (DL) techniques or radiomics features.[6-8] Moreover, a prediction model for RP after radiotherapy using computed tomography (CT) has been proposed.[9-12] Predicting RP using DL models is useful in making treatment decisions.

The dose–volume histogram (DVH) of the lung is the most common indicator for reducing RP occurrence. A correlation between DVH parameters and RP occurrence exists, the most important of which is V_{20} (the volume of the lung parenchyma that received ≥20 Gy).[2,13-15] To reduce the risk of developing grade ≥2 RP, V_{20} should be <30%–40%,[16,17] which is also adopted as a lung dose constraint in the National Comprehensive Cancer Network Guidelines. In addition, the

Access this article online

Quick Response Code:

Website: www.jmp.org.in

DOI: 10.4103/jmp.jmp_122_23

Address for correspondence: Mr. Takahiro Aoyama, Department of Radiation Oncology, Aichi Cancer Center, 1-1 Kanokoden, Chikusa-Ku, Nagoya, Aichi, 464-8681, Japan.
E-mail: aoyamat@aichi-cc.jp

How to cite this article: Aoyama T, Shimizu H, Koide Y, Kamezawa H, Fukunaga JI, Kitagawa T, *et al*. Deep learning-based lung dose prediction using chest x-ray images in non-small cell lung cancer radiotherapy. J Med Phys 2024;49:33-40.

dose should be lowered as much as possible (e.g., V_{20}<20%) for patients with originally compromised lung function, such as malignant pleural mesothelioma, after extrapleural pneumonectomy.[18,19] Therefore, it is necessary to create a treatment plan that reduces V_{20} as much as possible based on previous studies using DVH analysis.

Specifically, because chest X-ray images are the most frequently used and readily available radiological images, predicting V_{20} from these images is the simplest and most versatile method. However, to our knowledge, no studies have attempted this method. Thus, this study's primary objective was to develop a DL model using chest X-ray images to predict V_{20} of the lung following IMRT in patients with NSCLC. In addition, the secondary objective is to evaluate the prediction accuracy of the V_{20} using the DL model. Prediction of lung V_{20} promptly before treatment would be useful in selecting the optimal treatment technique. For example, if the predicted V_{20} is high, a preliminary decision can be made on whether to select a more advanced treatment technique (e.g., tumor tracking or proton beam therapy). In addition, it might be possible to avoid unnecessary CT scans (i.e., a simulated CT was taken but the lung dose was unacceptable and no radiation therapy was given).

Methods

Patient and treatment planning

Patients who had histologically confirmed NSCLC, had been irradiated with 60 Gy using IMRT between June 2018 and March 2022, and had undergone chest radiography on admission were included in the study [Figure 1]. This study was approved by the institutional review board of our institution (approval number: 2020-1-318). All patient data were fully anonymized, and all methods were performed in accordance with the relevant guidelines and regulations outlined by our institution.

Treatment planning

CT images were acquired using an Aquilion LB CT system (Canon Medical Systems, Tochigi, Japan) with a field of view of 550 cm × 550 cm, an image matrix of 512 × 512 pixels, and a slice thickness of 2.0 mm. For all patients, three scans of free breathing, inspiratory breathing, and expiratory breathing were performed, and the clinical target volume (CTV) was defined for all three phases according to the consensus guidelines.[20] The internal CTV (iCTV) was created by adding up the three CTVs, and a setup margin of 5 mm was added to the iCTV to create the planning target volume (PTV). The elective nodal region was not defined to prevent a pulmonary dose increase due to the extended radiation field.[21] To ensure consistency, target and normal tissue delineation were approved by an experienced radiation oncologist, according to the same treatment protocol for all patients.

The prescription dose for the PTV was 60 Gy in 30 fractions using the Varian TrueBeam system (Varian Medical Systems, Palo Alto, USA). The IMRT plans were created using one or two coplanar arcs with a photon energy beam of 6 MV by RayStation version 10.0 (RaySearch Laboratories AB, Stockholm, Sweden) using the calculation algorithm of the Collapsed Cone version 5.1. RaySearch Laboratories AB, Stockholm, Sweden). We calculated the lung dose parameters from the DVH of the treatment plan. All treatment plans were designed by medical physicists with ≥5 years of experience in IMRT planning and were of the highest quality with the normal lung, while other organs were at risk, dose values were kept as low as reasonably achievable.[22] These plans set the goals listed in Table 1.

Deep learning model

To construct and modify the DL model, a Windows PC with Intel Xeon 3.7 GHz, 32 GB RAM, and Neural Network Console (NNC) version 2.1 (Sony Corp., Tokyo, Japan) were used as a DL-integrated development environment.

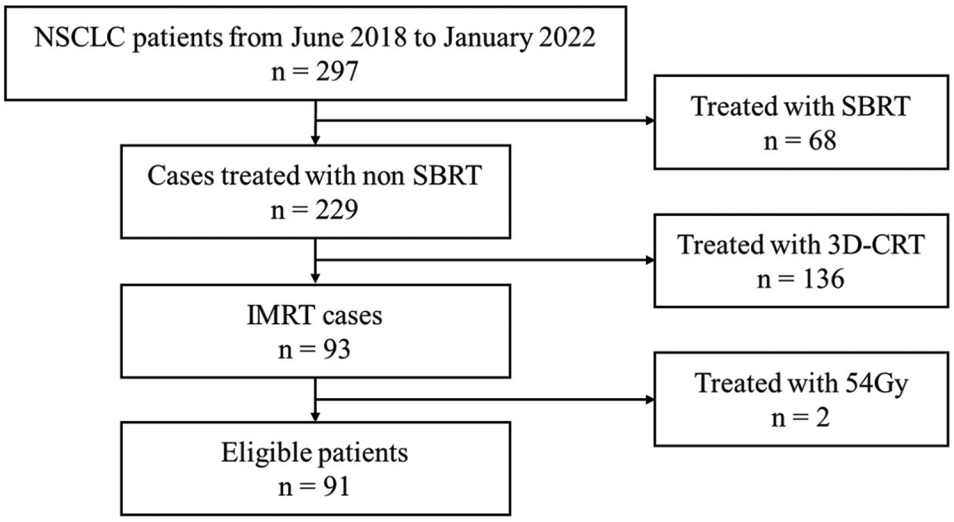

Figure 1: Selection of the study participants. 3D-CRT: Three-dimensional conformal radiotherapy, IMRT: Intensity-modulated radiotherapy, NSCLC: Nonsmall cell lung cancer, SBRT: Stereotactic radiotherapy

The convolutional neural network (CNN) architecture was used in this study [Figure 2], consisting of input, image augmentation, convolution, max pooling, rectified linear unit, batch normalization, affine, and Huber loss. Huber loss was calculated as follows:

$$Huber\ loss = \begin{cases} (x-y)^2, |x-y| < d \\ \delta\{2|x-y| - \delta\}, otherwise \end{cases} \quad (1)$$

where x is the predicted value and y is the true value.

All chest X-ray images were automatically resized to 64 × 64 pixels, and the format was changed from Digital Imaging and Communication in Medicine to Portable Network Graphics (8 bit). To reduce computational complexity, a resolution of 64 × 64 pixels has been selected in accordance with previous studies.[23,24] The resizing of images was conducted using the resizing function of NNC.

Image augmentation was used to address the limited number of patient images when building the CNN. The image augmentation parameters in the CNN were as follows: minimum scale, 0.9, maximum scale, 1.1; image angle, 0.1°, aspect ratio, 1.1; and image distortion, 0.1. Image augmentation was randomly applied to the input image to increase the size of the training set without acquiring new images. The parameters of the convolution layer used to extract features from an image were a kernel matrix of 3 × 3 pixels and padding and strides of 1. To reduce computational load and overfitting, max pooling was applied with 2 × 2 pixels. The rectified linear unit was used as a function, in which the output value was always 0 when the input value of the function was ≤0, and the output value was the same as the input value when the input value was >0. Normalization was performed between the layers of the neural network using batch normalization.

Affine was used as fully connected layers that combined all input values to all output layers. Huber loss was employed as a loss function to detect small errors using the squared error and large errors using the absolute error. This approach allowed for enhanced robustness to outliers. The optimizer parameters of the CNN for DL were calibrated as follows: learning rate, 0.001; optimizer, Adam ($\beta_1 = 0.9, \beta_2 = 0.999$); batch size, 8; and max epoch, 100. The computation time to execute the model is approximately 3 min.

Table 1: Clinical goals of treatment planning

Structure	Dosimetric parameter	Dose constraint
PTV	$D_{1\%}$ [Gy]	<63
	$D_{98\%}$ [Gy]	>57
iCTV	$D_{99\%}$ [Gy]	>54
Spinal cord	$D_{0.03cc}$ [Gy]	<48
Normal lungs minus iCTV	V_{20} [%]	<35
	V_5 [%]	<65
	Mean dose [Gy]	<20
Esophagus	$D_{0.03}$ [Gy]	<66
Heart	V_{45} [%]	<35
Brachial plexus	$D_{0.03cc}$ [Gy]	<66

Model evaluation and statistical analyses

The primary prediction outcome is V_{20}. We developed the DL model using a four-fold cross-validation approach, according to a previous study.[25] Figure 3 provides a visual representation of the pipeline, outlining the modeling process and evaluation. We divided the total data from June 2018 to March 2022 as follows: the training cohort consisted of data from June 2018 to June 2021 and the test cohort consisted of data from July 2021 to March 2022. The training cohort comprised 60 patients,

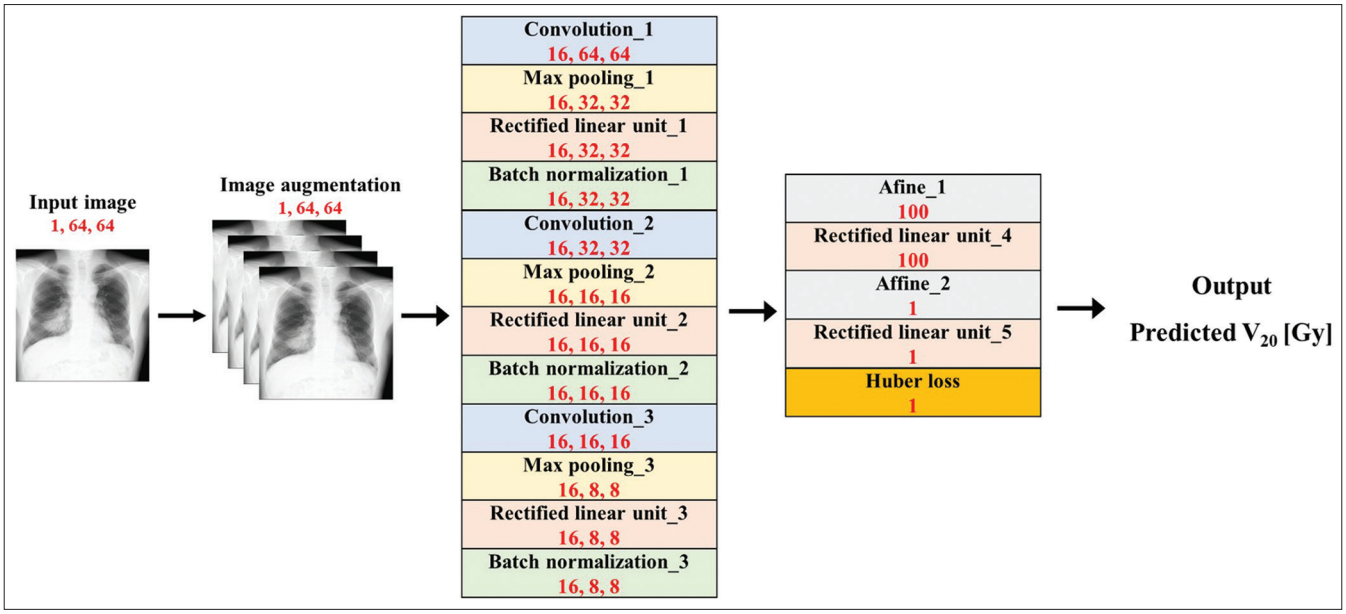

Figure 2: Multilayer neural network for the convolution layers used in this study. The red figures indicate the output size for each layer. For example, at the bottom of the first input layer, the three figures indicate the number of colors and the size (height and width) of the input image

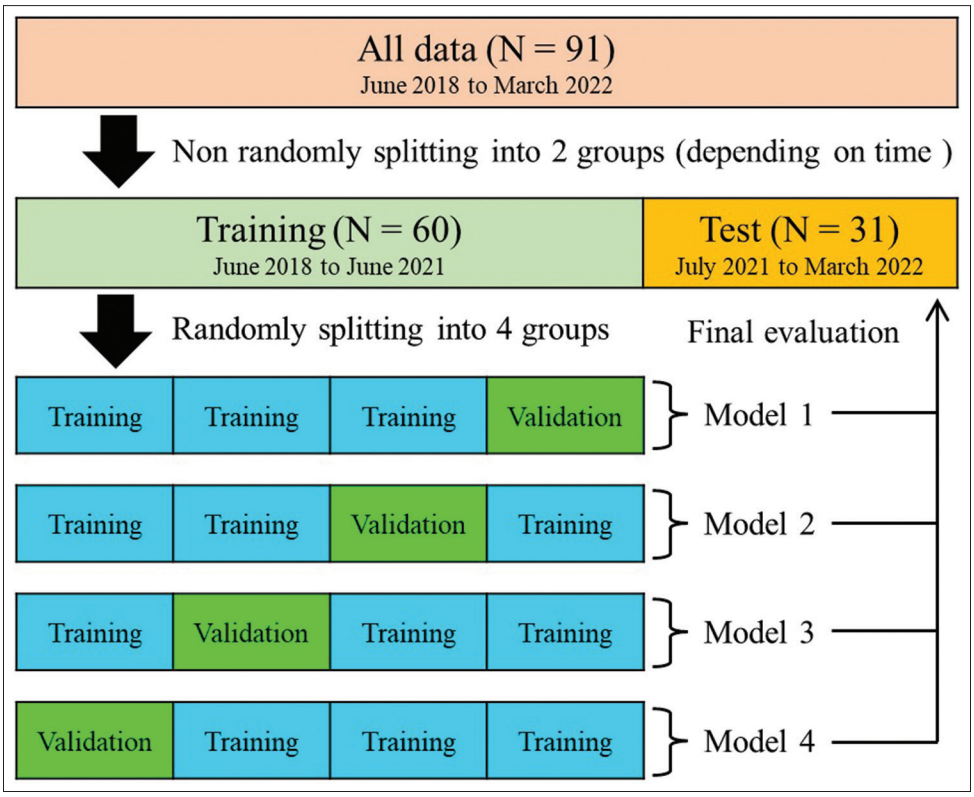

Figure 3: Four-fold cross-validation and test. The final predictive accuracy was calculated as the average value of the four models

randomly divided into four groups: patients 1–15, 16–30, 31–45, and 46–60. A regression model was trained using three of these groups, and the performance of the trained model was assessed using the remaining group for validation. The model, utilizing X-ray images and V20 in the training group, predicted and validated V_{20} values against the validation group. The secondary outcome is defined as the prediction accuracy of the DL model. The final predictive accuracy was the average value of the test data set. Furthermore, the prediction accuracy of the model was evaluated using the Pearson correlation coefficient, coefficient of determination (R^2), root mean square error (RMSE), and mean absolute error (MAE). In addition, as in the previous study,[23] we use the model as a binary classifier to determine if a patient would potentially receive V_{20}>20% or not. The sensitivity, specificity, and diagnostic accuracy were calculated as follows:

$$Sensitivity = TP / (TP + FN) \quad (2)$$

$$Specificity = TN / (FP + TN) \quad (3)$$

$$Diagnostic\ accuracy = (TP + TN) / (TP + TN + FP + FN) \quad (4)$$

where *TP* is the number of true positives, *FN* is the number of false negatives, *FP* is the number of false positives, and *TN* is the number of true negatives. In addition, the area under the receiver operator characteristic (ROC) and the area under the curve (AUC) were evaluated. Moreover, to investigate whether our DL model learns the size of lung tumors, we assessed prediction accuracy based on two factors: the primary tumor category (T2 ≤ or T3>, with sample sizes of 17 and 14) and the gross tumor volume (GTV). The test cohort's median GTV was 42.0 cm^3, divided into two groups: ≤42.0 cm^3 (sample size: 16) and >42.0 cm3 (sample size: 15). We calculated the RMSE for each individual sample and evaluated the differences in prediction accuracy using the Mann–Whitney *U*-test.

The prediction accuracy for V_5 and mean lung dose (MLD) were also evaluated as secondary outcomes. Statistical analysis was performed using EZR version 1.36,[26] a graphical user interface for R (The R Foundation for Statistical Computing, Vienna, Austria).

Results

Dataset

Table 2 shows the characteristics of the patients in the training and test cohorts. In the test cohort, the median V_{20}, V_5, and MLD were 19.0% (range, 4.9%–27.8%), 47.7% (range, 8.5%–59.2%), and 11.4 Gy (range, 2.9–16.2), respectively. Of the 91 patients, only 3 did not achieve the constraints of V_5 shown in Table 1 (V_5 = 75.5%, 67.1%, and 66.1%). Dose constraints other than V_5 were met in all patients.

Model performance

The developed model showed that the median predicted V_{20} was 16.5% (range, 8.2%–26.4%). Compared with the calculated V_{20}, the median prediction difference was − 1.8% (range, −13.0%–9.2%). The Pearson correlation coefficient

Table 2: Patient characteristics

Characteristic	Training (n=60)	Test (n=31)	Total (n=91)
Age			
Median [year]	70	72	71
Range	39–85	34–87	34–87
Sex			
Male (%)	42 (70.0)	23 (74.2)	65 (71.4)
Female (%)	18 (30.0)	8 (258)	26 (28.6)
Disease stage			
IIIA (%)	22 (36.7)	9 (30.0)	32 (35.2)
IIIB (%)	21 (35.0)	11 (36.7)	32 (35.2)
IIIC (%)	8 (13.3)	7 (23.3)	15 (16.4)
Other (%)	9 (15.0)	3 (10.0)	12 (13.2)
Tumor histologic type			
Squamous (%)	24 (40.0)	16 (51.6)	40 (44.0)
Nonsquamous (%)	36 (60.0)	15 (48.4)	51 (56.0)
Gross tumor volume			
Size [cm3]	28.4	42.0	39.2
Range	1.7–592.3	2.1–444.8	1.7–592.3
Combination therapy			
Chemotherapy (%)	58 (96.7)	29 (93.5)	87 (95.6)
Immunotherapy (%)	40 (66.7)	19 (61.3)	59 (64.8)
Radiation pneumonia			
< Grade 2 (%)	41 (68.3)	24 (77.4)	65 (71.4)
≥ Grade 2 (%)	19 (31.7)	7 (22.6)	26 (28.6)
V20			
Median [%]	19.9	19.0	19.3
Range	4.9–30.7	4.9–27.8	4.9–30.7
V5			
Median [%]	50.5	47.7	48.4
Range	14.4–75.5	8.5–59.2	8.5–75.5
MLD			
Median [Gy]	12.8	11.4	12.1
Range	3.7–17.7	2.9–16.2	2.9–17.7

between the calculated and predicted V_{20} was 0.40 ($P < 0.05$). The R^2, RMSE, and MAE values were 0.16, 5.4%, and 4.5%, respectively. Figure 4 shows the calculated–predicted plot. When binary classification was performed with V_{20}<20%, the model showed a sensitivity of 75.0% (6/8) (95% confidence interval [CI], 34.9–96.8), specificity of 82.6% (19/23) (95% CI, 61.2–95.0), and diagnostic accuracy of 80.6% (25/31) (95% CI, 62.5–92.5). Figure 5 shows the ROC curve for the predicted model. The AUC was 0.79 (95% CI, 0.60–0.97). The point at 19.7% was the best classification point, in which the sum values of the sensitivity and specificity were maximized. The Mann–Whitney *U* test results showed no significant difference in V_{20} prediction accuracy based on primary tumor category and GTV (P = 0.35 and 0.57, respectively).

In V_5 and MLD, the median prediction difference was 3.5% (range, −15.0–37.6) and 0.6 Gy (range, −4.0–5.3), respectively. The Pearson correlation coefficient, RMSE, and MAE for V_5 were 0.20 (P = 0.28), 14.9%, and 11.4%, respectively, and those for the MLD were 0.21 (P = 0.26), 3.2 Gy, and 2.7 Gy, respectively.

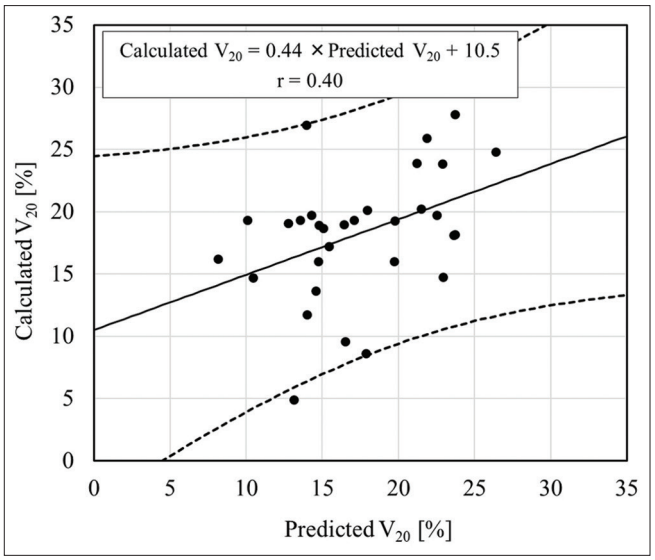

Figure 4: Scatter plot of the predicted V_{20} and calculated V_{20} (solid, regression line; dotted, 95% confidence interval line) V_{20}, volume of the lung parenchyma that received ≥20 Gy; *r*: Correlation coefficient

Discussion

In this study, a DL model was developed to predict V_{20} using the chest X-ray images of a patient. This model can predict V_{20} with a median difference of −1.8% (range, −13.0%–9.2%) and correlation coefficient of 0.40. To the best of our knowledge, only the study by Koide *et al*. predicted radiotherapy doses from X-ray images, which predicted cardiac doses for deep inspiration breath-hold (DIBH).[23] Their model predicted the amount of change in cardiac dose when DIBH was performed (correlation coefficient, 0.55). However, their model required frontal and lateral X-ray images in two directions, patient age, and body mass index. In contrast, our model is simpler and requires only frontal chest X-ray images. The ability to predict V_{20} before treatment planning will enable the selection of irradiation techniques for radiotherapy (e.g., tumor tracking and proton beam therapy). In addition, the dose to the normal lung should be reduced as much as possible, even if dose constraints are achieved. Dosage to the lung may be effectively reduced by referring to the V_{20} values predicted by the DL model together with the dose constraint values.

In contrast, we also found that the model's forecasting accuracy is still problematic, with a large error range of −13.0% to 9.2%. This estimate could potentially depend on any variability in the patient's inspiration percentage at the time of X-ray and CT image acquisition. In particular, the contribution to the error is expected to be significant because treatment planning is based on free-breathing CT images. CT imaging while monitoring the inspiratory rate using a respiratory monitoring system is expected

to improve accuracy. Furthermore, optimization of data augmentation is effective to ensure the robustness of the model[27] and the developed model will need to be re-examined in the future. In addition, the prediction accuracy of the model was found to be not significantly different depending on tumor size. This suggests that this DL model may be applicable to smaller tumor diameters, such as in stereotactic radiotherapy.

The prediction accuracies of V_5 and MLD were lower than V_{20}. Specifically, the RMSE for V_5 was 14.9%, which was worse than that for V_{20} (5.4%). The reason for this, besides the fact that this model is optimized for V_{20}, may be that the 5-Gy region is more widely distributed due to leakage doses from the multi-leaf collimator (MLC),[28] so prediction might be difficult. To increase the accuracy of V_5, adding the number of beams, rotation angle, and MLC transmittance parameters to the input of the DL model may improve the prediction accuracy of low doses spreading away from the tumor. Because of the correlations between parameters such as V_5, MLD, and RP occurrence,[29-31] creating optimized models for V_5 and MLD in the future is important.

Krafft *et al*. reported that the addition of pulmonary radiomics features to a prediction model for RP using CT improved the mean AUC from 0.51 to 0.66 with respect to predicting RP grade ≥3.[9] Kawahara *et al*. reported that multi-region radiomics analysis improved the accuracy of predicting grade ≥2 RP (mean AUC, 0.62–0.84).[12] Furthermore, Zhang *et al*. reported that by combining dose distribution maps with treatment planning CT images, they could predict postradiotherapy radiation pneumonitis with high accuracy (AUC = 0.7).[32] However, these models require CT images and specific regions of interest (ROI), which make segmentation time-consuming and less convenient. In addition, these models cannot be used for the purpose of assessing the suitability of radiotherapy before treatment planning. In contrast, because the chest X-ray DL model proposed herein does not require CT images or patient-specific ROI, prediction is easier and less time-consuming than when using CT images. Furthermore, by assessing the feasibility of radiotherapy based on V20 values before obtaining a treatment-planning CT scan, it may be possible to reduce unnecessary tests and costs. In addition, when a binary classification was performed with V_{20} <20% as the cutoff, the AUC was 0.79 (95% CI, 0.60–0.97), which is comparable to that in previous studies [Table 3]. The high AUC values suggest that when the developed model is used as a binary classifier, for example, even if the prepredicted values indicate V20 <20%, if the treatment planning system calculated values exceed 20%, it may contribute to further improvement in dose distribution. Although the developed model is not a predictive model for RP, V_{20} may be useful for predicting RP,[33,34] suggesting that the architecture of this model may be useful as a predictive model for future RP.

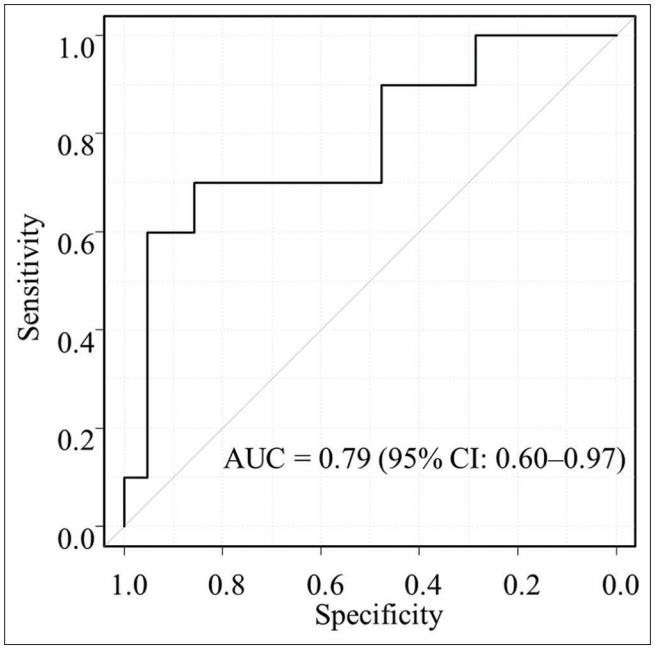

Figure 5: Receiver operating characteristic curves of the prediction models. When the cutoff was set as V_{20} <20%, the area under the curve score was 0.79. CI: Confidence interval

This study had some limitations. First, the proposed model was optimized to predict V_{20} rather than the RP. The predicted V_{20} can be used to determine the feasibility of radical irradiation or to determine the application of techniques that reduce the lung dose compared to conventional IMRT. In contrast, models that directly predict RP may be more valuable for predicting patient prognosis. Second, the single-center setting, small number of patients, lack of patients with V_{20} >35%, and varied patient backgrounds (such as concomitant therapy) are sources of bias. Future multicenter studies are required to reconstruct an RP prediction model.

Conclusions

Our DL model can predict V_{20} using chest X-ray images and plays an important role in the early determination of patient treatment strategies. It may be useful for determining

Table 3: Studies of deep learning models for predicting radiation therapy dose and clinical outcomes using digital imaging and communication in medicine images

References	Endpoint	DICOM images	Performance metrics
Koide *et al*.[23]	MHD	X-ray image (frontal and lateral)	r=0.55 AUC=0.864
Krafft *et al*.[9]	RP≥grade 3	CT image	AUC=0.66
Kawahara *et al*.[12]	RP≥grade 2	CT image	AUC=0.84
Zhang *et al*.[32]	RP≥grade 2	CT image	AUC=0.7
This study	Lung V20	X-ray image (frontal)	r=0.40 AUC=0.79

the treatment plan for patients and eliminating the need for unnecessary CT scans by enabling early dose prediction. Determining the treatment strategy using the proposed model leads to a reduction in the occurrence of grade ≥2 RP and maximizes the chance to follow PACIFIC regimens, including consolidation durvalumab, following definitive chemoradiotherapy. However, further research is needed to verify the robustness of the model and to further build RP prediction models.

Acknowledgments

The authors thank all the patients, investigators, and institutions involved in this study.

Financial support and sponsorship

This work was supported by Japan Society for the Promotion of Science (JSPS, Grant Number 23K14669).

Conflicts of interest

There are no conflicts of interest.

References

1. Peng J, Pond G, Donovan E, Ellis PM, Swaminath A. A comparison of radiation techniques in patients treated with concurrent chemoradiation for stage III non-small cell lung cancer. Int J Radiat Oncol Biol Phys 2020;106:985-92.
2. Chun SG, Hu C, Choy H, Komaki RU, Timmerman RD, Schild SE, *et al*. Impact of intensity-modulated radiation therapy technique for locally advanced non-small-cell lung cancer: A secondary analysis of the NRG oncology RTOG 0617 randomized clinical trial. J Clin Oncol 2017;35:56-62.
3. Antonia SJ, Villegas A, Daniel D, Vicente D, Murakami S, Hui R, *et al*. Durvalumab after chemoradiotherapy in stage III non-small-cell lung cancer. N Engl J Med 2017;377:1919-29.
4. Manav M, Goyal M, Kumar A, Arya AK, Singh H, Yadav AK. Deep learning approach for analyzing the COVID-19 chest X-rays. J Med Phys 2021;46:189-96.
5. Verma DK, Saxena G, Paraye A, Rajan A, Rawat A, Verma RK. Classifying COVID-19 and viral pneumonia lung infections through deep convolutional neural network model using Chest X-ray images. J Med Phys 2022;47:57-64.
6. Tamal M, Alshammari M, Alabdullah M, Hourani R, Alola HA, Hegazi TM. An integrated framework with machine learning and radiomics for accurate and rapid early diagnosis of COVID-19 from chest X-ray. Expert Syst Appl 2021;180:115152.
7. Zhang R, Tie X, Qi Z, Bevins NB, Zhang C, Griner D, *et al*. Diagnosis of coronavirus disease 2019 pneumonia by using chest radiography: Value of artificial intelligence. Radiology 2021;298:E88-97.
8. Zargari Khuzani A, Heidari M, Shariati SA. COVID-classifier: An automated machine learning model to assist in the diagnosis of COVID-19 infection in chest X-ray images. Sci Rep 2021;11:9887.
9. Krafft SP, Rao A, Stingo F, Briere TM, Court LE, Liao Z, *et al.* The utility of quantitative CT radiomics features for improved prediction of radiation pneumonitis. Med Phys 2018;45:5317-24.
10. Hao H, Zhou Z, Li S, Maquilan G, Folkert MR, Iyengar P, *et al*. Shell feature: A new radiomics descriptor for predicting distant failure after radiotherapy in non-small cell lung cancer and cervix cancer. Phys Med Biol 2018;63:095007.
11. Xie C, Yang P, Zhang X, Xu L, Wang X, Li X, *et al.* Sub-region based radiomics analysis for survival prediction in oesophageal tumours treated by definitive concurrent chemoradiotherapy. EBioMedicine 2019;44:289-97.
12. Kawahara D, Imano N, Nishioka R, Ogawa K, Kimura T, Nakashima T, *et al*. Prediction of radiation pneumonitis after definitive radiotherapy for locally advanced non-small cell lung cancer using multi-region radiomics analysis. Sci Rep 2021;11:16232.
13. Tsujino K, Hashimoto T, Shimada T, Yoden E, Fujii O, Ota Y, *et al*. Combined analysis of V20, VS5, pulmonary fibrosis score on baseline computed tomography, and patient age improves prediction of severe radiation pneumonitis after concurrent chemoradiotherapy for locally advanced non-small-cell lung cancer. J Thorac Oncol 2014;9:983-90.
14. Marks LB, Bentzen SM, Deasy JO, Kong FM, Bradley JD, Vogelius IS, *et al.* Radiation dose-volume effects in the lung. Int J Radiat Oncol Biol Phys 2010;76:S70-6.
15. Tsujino K, Hirota S, Endo M, Obayashi K, Kotani Y, Satouchi M, *et al.* Predictive value of dose-volume histogram parameters for predicting radiation pneumonitis after concurrent chemoradiation for lung cancer. Int J Radiat Oncol Biol Phys 2003;55:110-5.
16. Graham MV, Purdy JA, Emami B, Harms W, Bosch W, Lockett MA, *et al*. Clinical dose-volume histogram analysis for pneumonitis after 3D treatment for non-small cell lung cancer (NSCLC). Int J Radiat Oncol Biol Phys 1999;45:323-9.
17. Ramella S, Trodella L, Mineo TC, Pompeo E, Stimato G, Gaudino D, *et al.* Adding ipsilateral V20 and V30 to conventional dosimetric constraints predicts radiation pneumonitis in stage IIIA-B NSCLC treated with combined-modality therapy. Int J Radiat Oncol Biol Phys 2010;76:110-5.
18. Ahamad A, Stevens CW, Smythe WR, Vaporciyan AA, Komaki R, Kelly JF, *et al.* Intensity-modulated radiation therapy: A novel approach to the management of malignant pleural mesothelioma. Int J Radiat Oncol Biol Phys 2003;55:768-75.
19. Allen AM, Czerminska M, Jänne PA, Sugarbaker DJ, Bueno R, Harris JR, *et al.* Fatal pneumonitis associated with intensity-modulated radiation therapy for mesothelioma. Int J Radiat Oncol Biol Phys 2006;65:640-5.
20. Nestle U, De Ruysscher D, Ricardi U, Geets X, Belderbos J, Pöttgen C, *et al.* ESTRO ACROP guidelines for target volume definition in the treatment of locally advanced non-small cell lung cancer. Radiother Oncol 2018;127:1-5.
21. Schild SE, Pang HH, Fan W, Stinchcombe TE, Vokes EE, Ramalingam SS, *et al*. Exploring radiotherapy targeting strategy and dose: A pooled analysis of cooperative group trials of combined modality therapy for stage III NSCLC. J Thorac Oncol 2018;13:1171-82.
22. Shimizu H, Sasaki K, Aoyama T, Iwata T, Kitagawa T, Kodaira T. Lung dose reduction in patients with stage III non-small-cell lung cancer using software that estimates patient-specific dose reduction feasibility. Phys Med 2021;85:57-62.
23. Koide Y, Aoyama T, Shimizu H, Kitagawa T, Miyauchi R, Tachibana H, *et al*. Development of deep learning chest X-ray model for cardiac dose prediction in left-sided breast cancer radiotherapy. Sci Rep 2022;12:13706.
24. Shelke A, Inamdar M, Shah V, Tiwari A, Hussain A, Chafekar T, *et al*. Chest X-ray classification using deep learning for automated COVID-19 screening. SN Comput Sci 2021;2:300.
25. Koide Y, Shimizu H, Wakabayashi K, Kitagawa T, Aoyama T, Miyauchi R, et al. Synthetic breath-hold CT generation from free-breathing CT: A novel deep learning approach to predict cardiac dose reduction in deep-inspiration breath-hold radiotherapy. J Radiat Res 2021;62:1065-75.
26. Kanda Y. Investigation of the freely available easy-to-use software 'EZR' for medical statistics. Bone Marrow Transplant 2013;48:452-8.
27. Nemoto T, Futakami N, Kunieda E, Yagi M, Takeda A, Akiba T, *et al.* Effects of sample size and data augmentation on U-Net-based automatic segmentation of various organs. Radiol Phys Technol 2021;14:318-27.
28. Murshed H, Liu HH, Liao Z, Barker JL, Wang X, Tucker SL, *et al.* Dose and volume reduction for normal lung using intensity-modulated radiotherapy for advanced-stage non-small-cell lung cancer. Int J Radiat Oncol Biol Phys 2004;58:1258-67.
29. Wang W, Xu Y, Schipper M, Matuszak MM, Ritter T, Cao Y, *et al.* Effect of normal lung definition on lung dosimetry and lung toxicity prediction in radiation therapy treatment planning. Int J Radiat Oncol Biol Phys

2013;86:956-63.
30. Hernando ML, Marks LB, Bentel GC, Zhou SM, Hollis D, Das SK, *et al*. Radiation-induced pulmonary toxicity: A dose-volume histogram analysis in 201 patients with lung cancer. Int J Radiat Oncol Biol Phys 2001;51:650-9.
31. Fay M, Tan A, Fisher R, Mac Manus M, Wirth A, Ball D. Dose-volume histogram analysis as predictor of radiation pneumonitis in primary lung cancer patients treated with radiotherapy. Int J Radiat Oncol Biol Phys 2005;61:1355-63.
32. Zhang Z, Wang Z, Luo T, Yan M, Dekker A, De Ruysscher D, *et al*. Computed tomography and radiation dose images-based deep-learning model for predicting radiation pneumonitis in lung cancer patients after radiation therapy. Radiother Oncol 2023;182:109581.
33. Su M, Miften M, Whiddon C, Sun X, Light K, Marks L. An artificial neural network for predicting the incidence of radiation pneumonitis. Med Phys 2005;32:318-25.
34. Luna JM, Chao HH, Diffenderfer ES, Valdes G, Chinniah C, Ma G, *et al.* Predicting radiation pneumonitis in locally advanced stage II-III non-small cell lung cancer using machine learning. Radiother Oncol 2019;133:106-12.